

Superdiffusion and Non-Gaussian Statistics in a Driven-Dissipative 2D Dusty Plasma

Bin Liu and J. Goree

Department of Physics and Astronomy, The University of Iowa, Iowa City, Iowa 52242, USA

(Received 1 June 2007; published 6 February 2008)

Anomalous diffusion and non-Gaussian statistics are detected experimentally in a two-dimensional driven-dissipative system. A single-layer dusty plasma suspension with a Yukawa interaction and frictional dissipation is heated with laser radiation pressure to yield a structure with liquid ordering. Analyzing the time series for mean-square displacement, superdiffusion is detected at a low but statistically significant level over a wide range of temperatures. The probability distribution function fits a Tsallis distribution, yielding q , a measure of nonextensivity for non-Gaussian statistics.

DOI: [10.1103/PhysRevLett.100.055003](https://doi.org/10.1103/PhysRevLett.100.055003)

PACS numbers: 52.27.Lw, 52.27.Gr, 82.70.Dd

Two-dimensional (2D) physical systems with a single-layer of mutually interacting particles include a Wigner lattice of electrons on a liquid helium surface [1], ions confined magnetically in a Penning trap [2], colloidal suspensions [3], vortex arrays in the mixed state of type-II superconductors [4], and dusty plasmas levitated in a single layer [5]. Within biological cell membranes, proteins can undergo 2D diffusion [6].

We investigate random motion in driven-dissipative 2D liquids. In experiments with a single-layer dusty plasma suspension, particles interact with a Yukawa potential [7] and are damped by gas friction. Like 2D granular media [8], our particles are driven by an external source, and their average kinetic energy is set by a balance of driving forces and dissipation.

Random motion is characterized using the mean-square displacement (MSD) time series and the probability distribution function (PDF). We define these separately for the x and y directions. For the x direction, MSD is $\langle [x(\Delta t) - x(0)]^2 \rangle$, and PDF is the histogram of $|x(\tau) - x(0)|$ evaluated at a specified delay τ . Random motion characterized as pure diffusion has two signatures: having a PDF that is Gaussian at all times [9], and obeying the Einstein relation $\lim_{t \rightarrow \infty} \langle [x(\Delta t) - x(0)]^2 \rangle = 2D\Delta t$ [10] at long times, where D is a diffusion constant.

Anomalous diffusion is a term used to describe motion that is found empirically to not exhibit these signatures. In this case, Fick's law is not satisfied, and there is no constant diffusion coefficient. Anomalous diffusion is associated with non-Gaussian statistics sometimes, as in a liquid with vortices [11,12], but not always [13].

Non-Gaussian statistics, which are often exhibited by nonequilibrium systems, can follow a Tsallis distribution for a random variable z , for example, displacement of a particle [14]

$$[1 - \beta(1 - q)z^2]^{1/(1-q)}, \quad (1)$$

where the nonextensivity parameter q is $q = 1$ for Gaussian and $q \neq 1$ for non-Gaussian statistics. In addition to anomalous diffusion, Tsallis statistics has been used to describe turbulence in pure electron plasmas [15].

There is a disagreement in the literature regarding whether motion can ever be purely diffusive in 2D liquids. There are simulations and theories predicting that motion is not diffusive for any type of interparticle interaction [16,17]. On the other hand, some recent simulations [18,19] have found signatures of diffusion in 2D liquids near the disordering transition, for various interparticle interactions. All these simulations can have limitations, including a finite system size.

The literature for diffusion in 2D liquids includes mostly simulations of simple liquids. Experiments with 2D liquids are fewer, including soft matter systems such as colloidal suspensions [20], granular material [21], and dusty plasmas [12,22–24]. Distinguishing diffusion from weakly anomalous diffusion at a statistically significant level requires large data sets for long times, which can be hard in a simulation [13] and even harder in an experiment due to a limited thread lifetime. Here, the term “thread” refers to a time series of position measurements for one particle.

Two-dimensional transport has been experimentally studied in dusty plasmas consisting of partially ionized rarefied gas that fills a 3D volume and contains charged microspheres suspended in a single thin layer. Juan *et al.* [23] measured the MSD transverse to a sheared flow in a quasi-2D multilayer suspension, and reported a diffusion coefficient that increased with the laser power that generated the shear. Nunomura *et al.* [24] reported D for a layer that was perturbed by unstable movement of a few heavier particles in an incomplete second layer thereby raising the suspension kinetic temperature, T ; they interpreted their results as indicating diffusion, with $D \propto T$. Ratynskaia *et al.* [12] used a smaller cluster of microspheres suspended in a single layer that was heated presumably by instabilities in the dusty plasma; they described their motion as superdiffusion, characterized by Lévy statistics, driven by flows [12,23]. There have also been other dusty plasma experiments to measure shear [5,25] and thermal conduction [26,27]. These experiments can be compared with 2D granular medium experiments, which are also driven dissipative, and where diffusion takes a different character if there is a flow [28].

Here we report an experimental study of 2D diffusion with a different heating method. Our dusty plasma had no second layer [24], and we used a laser heating scheme, configured to avoid shear and macroscopic flows [12,23]. The method provides steady conditions, allowing us to record large data sets to provide a low detection limit for superdiffusion.

Our laser-heated suspension is a driven-dissipative system. Radiation pressure forces from rastered cw laser beams apply strong kicks in the $\pm x$ directions to a few particles at a time, and these collide with other particles to thermalize the motion. Energy input from the laser is ultimately balanced by dissipation on the neutral gas [29], allowing a steady-state energy balance. Particles receive random kicks more often from collisions with other particles than from the laser beams.

We used a radio-frequency (rf) apparatus [30], Fig. 1(a). Plasma was formed from Ar at 8.6 mTorr by applying 13.56 MHz rf, yielding a dc self-bias of -95 V. We

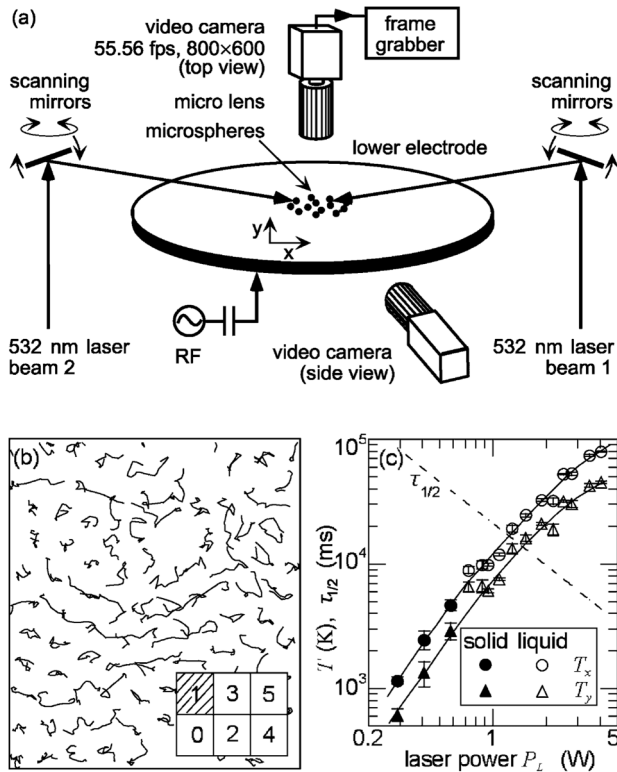


FIG. 1. (a) Apparatus. An argon plasma is formed in a vacuum chamber, not shown here. Microspheres suspended in a single layer above a lower electrode are kicked by a pair of rastered laser beams. (b) Particle trajectories for $P_L = 2.5$ W in cell 1. We divide the camera's full field-of-view (FOV) into 6 cells, as shown in the inset. Motion is mostly ballistic in the 0.5 s time interval shown here. (c) Heating. Kinetic temperatures, averaged over the full FOV, increase with P_L . Structures with $G_\theta < 0.1$ were identified as liquid and lacked large crystalline domains; structures identified as solid were not defect-free. At higher temperatures, threads have a shorter half-life $\tau_{1/2}$. The anisotropy $T_x > T_y$ is due to laser heating.

introduced >6000 polymer microspheres, $4.83 \pm 0.08 \mu\text{m}$ in diameter, to form a single layer. The particles experienced a damping rate $\nu_E = 2.5 \text{ s}^{-1}$ [29]. A cooled camera recorded 37 s movies of particle motion at 55.56 frames per second; its field-of-view (FOV) of $14.8 \times 10.8 \text{ mm}^2$ included about 900 particles in the central portion of the suspension. A 0.1 W Ar^+ laser beam swept horizontally once per exposure illuminate particles. We verified that conditions remained steady throughout the experiment, and using a side-view camera we verified that no out-of-plane buckling occurred.

We analyzed movies, making $>2 \times 10^7$ particle positions (x, y) using the moment method, optimized as in [31]. Tracking particles from frame to frame yields their trajectories, i.e., threads, Fig. 1(b). Threads have a finite half-life $\tau_{1/2}$, Fig. 1(c), due to particles exiting the FOV or becoming indistinguishable during tracking. Lacking hydrodynamic coupling to any nearby wall, our suspension rotated as a rigid body when it was in a solid state. We always subtract this global rotation motion before calculating other quantities. We report temperatures T_x and T_y computed from mean-square velocities.

The Wigner-Seitz radius [32] was $a = 0.24 \text{ mm}$. The particle charge $Q/e = -5700$ and screening parameter $a/\lambda_D = 0.90$ were measured using the natural phonon method [24]. Repeated measurements of Q and a/λ_D had a 4% dispersion. We calculated a time scale [32] $\omega_{pd}^{-1} = 9.2 \text{ ms}$.

To provide a well-controlled and adjustable particle kinetic temperature without affecting Q or a/λ_D , we used the laser-heating method of [30]. A pair of 532 nm cw laser beams directed in the $\pm x$ directions drew Lissajous figures with frequencies $f_x = 40.451 \text{ Hz}$ and $f_y = 25 \text{ Hz}$ in a 16.2 mm wide rectangular stripe spanning

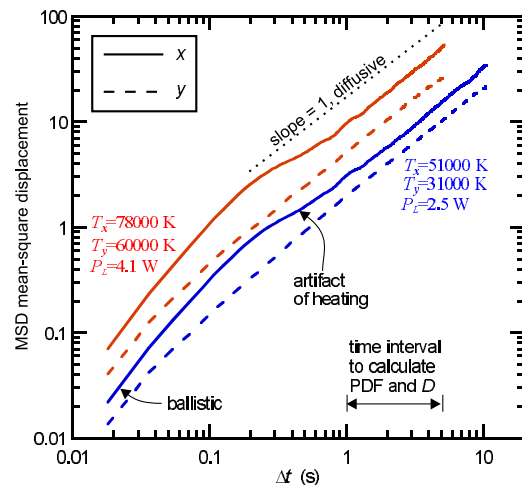


FIG. 2 (color online). MSD, averaged over threads and overlapping time segments [34], computed separately for x and y . Data here are for two laser powers. The MSD in the x direction is larger than that in the y direction, due to $T_x > T_y$. Distance is normalized by the Wigner-Seitz radius a .

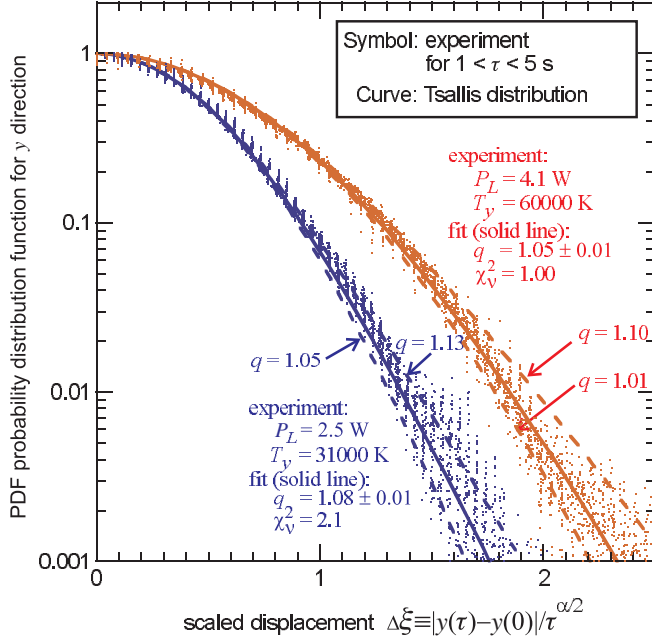


FIG. 3 (color online). PDF for the y direction, and the same conditions as in Fig. 2. Self-similarity is revealed by the collapse of PDFs at successive delays τ , with the scaled displacement $\Delta\xi \equiv |y(\tau) - y(0)|/\tau^{\alpha/2}$. Fitting to Eq. (1) yields the smooth solid curves and the measure of nonextensivity q . Other curves shown bracket the smooth curve for the fit.

the entire suspension in the x direction. We adjusted the temperature by varying the laser power, Fig. 1(c). Gradually increasing the power of each beam to $P_L = 0.75$ W, as measured in the chamber, we melted the solid, as judged by G_θ [33] and $g(r)$ [30]. Flow velocities were $< 8\%$ of the thermal velocity.

Compared to [30], different Lissajous frequencies and a wider stripe helped reduce coherent modes and nonuniformities in the laser heating. Coherent modes, excited by the finite frequency of the laser-beam's repetitive motion, represented 10% of the total power for the x direction, and 6% for the y direction. We measure T and analyze random motion in each of six portions of the FOV, i.e., cells, in Fig. 1(b) inset; this method reduces the effect of a 35%

spatial variation of temperature over the full FOV. Due to the anisotropic momentum input from our two laser beams, T_x exceeded T_y , Fig. 1(c), with T_x/T_y as large as 1.8.

The MSD, Fig. 2, exhibits ballistic motion at short time, $\Delta t < 0.1$ s. For the x direction, the MSD also exhibits an artifact of laser heating between 0.1 and 1.0 s. Heating in the y direction arises only from collisions, so that it lacks this artifact, leading us to analyze motion mostly in the y direction. The MSD is always larger in the x direction, due to $T_x > T_y$. Here, we are interested in long-time behavior, characterized by measuring the diffusion exponent α [13], which we present later.

The PDF has a self-similar form, as demonstrated in Fig. 3 by the collapse of PDF curves at successive delays τ ranging from 1 to 5 s. We scaled the displacement as $\Delta\xi \equiv |y(\tau) - y(0)|/\tau^{\alpha/2}$ to yield a self-similar form.

A Tsallis distribution fits our self-similar PDF, and this fit yields q . Recall that Gaussian statistics would be indicated by $q = 1$. For the lower laser power in Fig. 3, we found $q = 1.08 \pm 0.01$; for the higher power we found $q = 1.05 \pm 0.01$. Repeating this analysis for other temperatures, and averaging the resulting q values within a temperature range, yields \bar{q} in Table I.

We observe $\bar{q} > 1$, i.e., non-Gaussian statistics for all temperature ranges. These results are statistically significant, with a confidence level $> 95\%$ for rejecting the null hypothesis $\bar{q} \leq 1$. The deviation from Gaussian statistics is greatest in our lowest temperature range, near the disordering transition. Unlike [12], where a deviation from Gaussian statistics was attributed to prominent vortex flows, our experiment was prepared without vortices.

By calculating the diffusion exponent α , we determined that random motion exhibits superdiffusion. In this test, we fit MSD for displacements in the y direction to the scaling $(\Delta t)^\alpha$, yielding a measurement of α_y for different ranges of T_y and Δt . We then averaged the resulting α_y values over ranges of T_y and time delay. In Table I, we report this mean value $\bar{\alpha}_y$ and a standard deviation of the mean. In all cases, we find $\bar{\alpha}_y > 1$, i.e., superdiffusion, as compared with $\alpha = 1$ reported in [24]. The level of superdiffusion, $\bar{\alpha}_y - 1$, is small, but statistically significant. Using our large data sets

TABLE I. The measure \bar{q} of nonextensivity indicates non-Gaussian statistics. Mean diffusion exponent $\bar{\alpha}_y$ (and p value for testing the null hypothesis that there is no superdiffusion) indicates superdiffusion.

	Time Delay (s)	Temperature Range T_y (10^3 K)		
		10–20	20–40	40–60
\bar{q}	$1 < \tau < 5$	1.20 ± 0.09	1.11 ± 0.06	1.05 ± 0.02
$\bar{\alpha}_y$	$1 < \Delta t < 5$	1.052 ± 0.019	1.059 ± 0.011	1.009 ± 0.011
p		0.007	2×10^{-5}	0.210
$\bar{\alpha}_y$	$5 < \Delta t < 9$	1.088 ± 0.048	1.082 ± 0.040	
p		0.042	0.038	
$\bar{\alpha}_y$	$9 < \Delta t < 13$	1.146 ± 0.062		
p		0.028		
$\bar{\alpha}_y$	$13 < \Delta t < 17$	1.183 ± 0.064		
p		0.006		

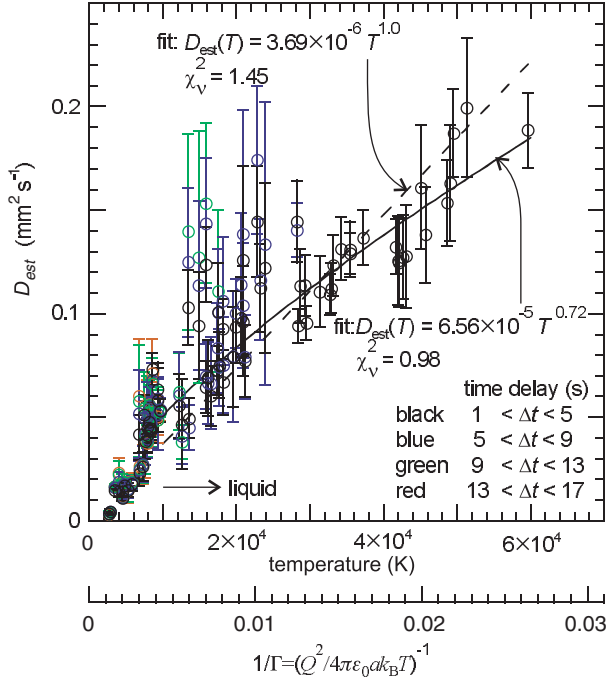


FIG. 4 (color online). Temperature dependence of D_{est} calculated from $\langle (y(\Delta t) - y(0))^2 \rangle / 2\Delta t$. The smooth curve is a fit, weighted by error bars, of data for a liquid. Scatter is due to finite time interval and number of threads.

and the student's t test, we can reject the null hypothesis that $\bar{\alpha}_y \leq 1$ with a confidence level of $>95\%$ (i.e., $p < 0.05$) in all cases except possibly the highest temperature range in Table I.

The level of superdiffusion we detected did not reach the larger values of $\alpha > 1.1$ observed in equilibrium 2D Yukawa simulations [13]. Like our experiment, these simulations have no flows and no incomplete second layer, but they differ by assuming an energy equilibrium with no friction. We speculate that friction may suppress superdiffusion. Experimental systems experience friction, more strongly for colloids which are overdamped, and less strongly for dusty plasma, which uses a rarefied gas rather than a liquid solvent.

Finally, we use our large data sets to investigate whether the MSD in our 2D liquid can yield a diffusion coefficient that has the scaling with temperature previously reported for an experiment [24]. We tentatively calculate an estimated diffusion coefficient D_{est} as $\langle (y(\Delta t) - y(0))^2 \rangle / 2\Delta t$ for displacement in the y direction, averaged for all movies and for various time delays Δt , yielding Fig. 4. This coefficient of course increases with temperature. Based on a smaller data set, it was reported [24] that in a liquid this increase fits a straight line with an intercept on the horizontal axis at the melting temperature. However, we found that such a line fits our data more poorly ($\chi_v^2 > 4$) than a power law ($\chi_v^2 = 0.98$) or a straight line through the origin ($\chi_v^2 = 1.45$).

We thank Z. Donkó, V. Nosenko, J. Scudder, and F. Skiff for helpful discussions. Work supported by NASA and DOE.

- [1] C. C. Grimes and G. Adams, Phys. Rev. Lett. **42**, 795 (1979).
- [2] T. B. Mitchell *et al.*, Phys. Plasmas **6**, 1751 (1999).
- [3] C. A. Murray, W. O. Sprenger, and R. A. Wenk, Phys. Rev. B **42**, 688 (1990).
- [4] P. L. Gammel *et al.*, Phys. Rev. Lett. **59**, 2592 (1987).
- [5] V. Nosenko and J. Goree, Phys. Rev. Lett. **93**, 155004 (2004).
- [6] K. Jacobson, E. D. Sheets, and R. Simson, Science **268**, 1441 (1995).
- [7] U. Konopka, G. E. Morfill, and L. Ratke, Phys. Rev. Lett. **84**, 891 (2000).
- [8] F. Rouyer and N. Menon, Phys. Rev. Lett. **85**, 3676 (2000).
- [9] D. del-Castillo-Negrete, Phys. Fluids **10**, 576 (1998).
- [10] A. Einstein, Ann. Phys. (Leipzig) **322**, 549 (1905).
- [11] T. H. Solomon, E. R. Weeks, and H. L. Swinney, Phys. Rev. Lett. **71**, 3975 (1993).
- [12] S. Ratynskaia *et al.*, Phys. Rev. Lett. **96**, 105010 (2006).
- [13] B. Liu and J. Goree, Phys. Rev. E **75**, 016405 (2007).
- [14] C. Tsallis *et al.*, Phys. Rev. Lett. **75**, 3589 (1995).
- [15] B. M. Boghosian, Phys. Rev. E **53**, 4754 (1996).
- [16] M. H. Ernst, E. H. Hauge, and J. M. J. Van Leeuwen, Phys. Rev. Lett. **25**, 1254 (1970).
- [17] B. J. Alder and T. E. Wainwright, Phys. Rev. A **1**, 18 (1970).
- [18] D. N. Perera and P. Harrowell, Phys. Rev. Lett. **81**, 120 (1998).
- [19] B. Liu, J. Goree, and O. S. Vaulina, Phys. Rev. Lett. **96**, 015005 (2006).
- [20] A. H. Marcus, B. H. Lin, and S. A. Rice, Phys. Rev. E **53**, 1765 (1996).
- [21] R. D. Wildman, J. M. Huntley, and J.-P. Hansen, Phys. Rev. E **60**, 7066 (1999).
- [22] W. T. Juan and L. I., Phys. Rev. Lett. **80**, 3073 (1998).
- [23] W. T. Juan, M. H. Chen, and L. I., Phys. Rev. E **64**, 016402 (2001).
- [24] S. Nunomura *et al.*, Phys. Rev. Lett. **96**, 015003 (2006).
- [25] V. E. Fortov, O. S. Vaulina, and O. F. Petrov, Plasma Phys. Controlled Fusion **47**, B551 (2005).
- [26] S. Nunomura *et al.*, Phys. Rev. Lett. **95**, 025003 (2005).
- [27] V. E. Fortov *et al.*, Phys. Rev. E **75**, 026403 (2007).
- [28] Brian Utter and R. P. Behringer, Phys. Rev. E **69**, 031308 (2004).
- [29] B. Liu, J. Goree, V. Nosenko, and L. Boufendi, Phys. Plasmas **10**, 9 (2003).
- [30] V. Nosenko, J. Goree, and A. Piel, Phys. Plasmas **13**, 032106 (2006).
- [31] Y. Feng, J. Goree, and B. Liu, Rev. Sci. Instrum. **78**, 053704 (2007).
- [32] G. J. Kalman *et al.*, Phys. Rev. Lett. **92**, 065001 (2004).
- [33] P. Hartmann *et al.*, Phys. Rev. E **72**, 026409 (2005).
- [34] M. J. Saxton, Biophys. J. **72**, 1744 (1997).